Direct Power Control of Grid-Connected Wound Rotor Induction Machine Without Rotor Position Sensors

Rajib Datta and V. T. Ranganathan, *Senior Member, IEEE*

Abstract—A method is presented for fast response control of the torque and flux of a grid connected wound rotor induction machine fed by back to back connected voltage source inverters on the rotor side. It is based on the measurement of active and reactive power on the grid side where voltages and currents are alternating at fixed frequency. The active and reactive powers are made to track references using hysteresis controllers. The method eliminates the need for rotor position sensing and gives excellent dynamic performance, as shown by simulation and experimental results from a variable speed constant frequency induction generator system. It is also capable of starting on the fly. It is thus an attractive sensorless control method for drive as well as generator applications.

Index Terms—Induction motors, power control, reactive power control, sensorless control, torque control, variable speed constant frequency applications, variable speed drives, wind power generation.

NOMENCLATURE

ψ_s, ψ_r, ψ_m	Stator flux, rotor flux and air-gap flux, respectively.
i_s, i_r	Stator current and rotor current, respectively.
u_s, u_r	Stator voltage and rotor voltage, respectively.
i_{sq}, i_{sd}	Active component and reactive component of stator current, respectively.
i_{rq}, i_{rd}	Active component and reactive component of rotor current, respectively.
i_{ms}	Stator flux magnetizing current.
δ_p	Angle between the stator flux and rotor flux.
ω_s	Stator frequency.
L_0	Magnetizing inductance.
σ_s, σ_r	Stator and rotor leakage factors, respectively.
P_s, P_r	Stator and rotor active powers, respectively.
Q_s, Q_r	Stator and rotor reactive powers, respectively.
P, Q	Total active and reactive powers, respectively.
m_d	Machine torque.

I. INTRODUCTION

IN RECENT years, there has been an increased attention toward wind power generation. Conventionally, grid-connected cage rotor induction machines are used as wind gen-erators at medium power level. When connected to the constant frequency network, the induction generator runs at near-synchronous speed drawing the magnetizing current from the mains, thereby resulting in constant speed constant frequency (CSCF) operation. However, the power capture due to fluctuating wind speed can be substantially improved if there is flexibility in varying the shaft speed.

In such variable speed constant frequency (VSCF) application rotor side control of grid-connected wound rotor induction machine is an attractive solution. In the system under consideration, the stator is directly connected to the three phase grid and the rotor is supplied by two back-to-back PWM converters (Fig. 1). Such an arrangement provides flexibility of operation in subsynchronous and supersynchronous speeds both in the generating and motoring modes. The rating of the power converters used in the rotor circuit is substantially lower than the machine rating and is decided by the range of operating speed. Of the two converters, the function of the line side converter is to regulate the dc bus voltage and act as unity power factor interface to the grid for either direction of power flow. The machine side converter has to control the torque and flux of the machine or alternatively the active and reactive powers. The present work is concerned with the control of the machine side converter.

The conventional approach for independent control of active and reactive powers handled by the machine is stator flux oriented vector control with rotor position sensors [1], [2]. The performance of the system in this case depends on the accuracy of computation of the stator flux and the accuracy of the rotor position information derived from the position encoder. Alignment of the position sensor is moreover, difficult in a doubly-fed wound rotor machine.

Position sensorless vector control methods have been proposed by several research groups in the recent past [3]–[6]. In [3], a dynamic torque angle controller is proposed. This method uses integration of the PWM rotor voltage to compute the rotor flux; hence satisfactory performance cannot be achieved at or near synchronous speed. Most of the other methods proposed make use of the measured rotor current and use coordinate transformations for estimating the rotor position [4]–[6]. Varying degree of dependence on machine parameters is observed in all these strategies.

Alternative approaches to field oriented control such as direct self control (DSC) [7] and direct torque control (DTC) [8], [9] have been proposed for cage rotor induction machines. In these strategies, two hysteresis controllers, namely a torque controller and a flux controller, are used to determine the instantaneous
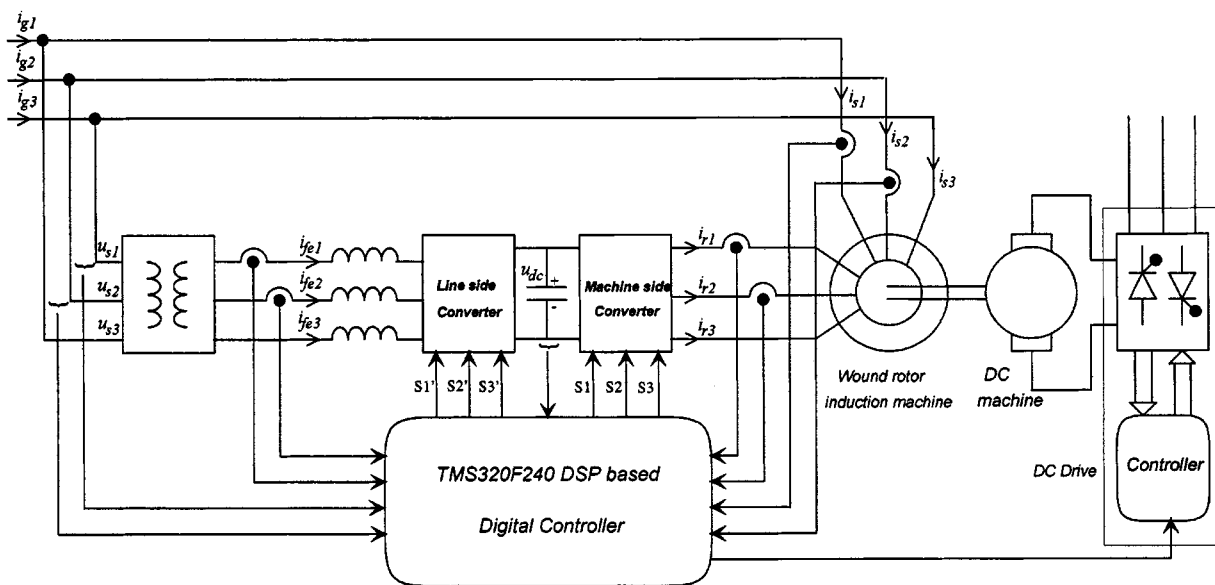
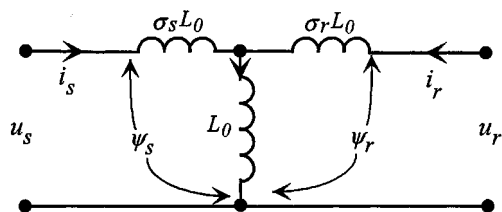Fig. 1.   Schematic block diagram of the experimental setup.
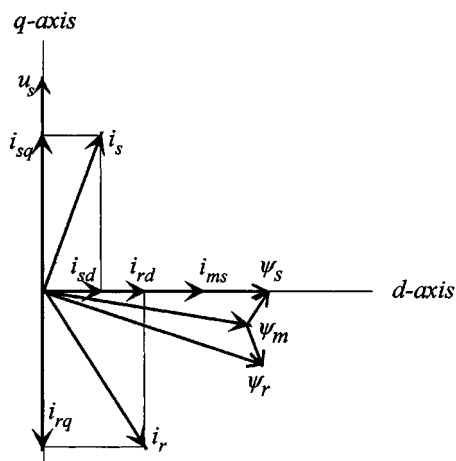
Fig. 2.   Approximate equivalent circuit.

Fig. 3.   Phasor diagram.

switching state for the inverter. These methods of control are computationally very simple and do not require rotor position information. However, the application of such techniques to the control of wound rotor induction machine has not been considered so far.

In this paper, a recently developed algorithm [10], [11] for independent control of active and reactive powers with high dynamic response in case of a wound rotor induction machine is described. The instantaneous switching state of the rotor side converter is determined based on the active and reactive powers

measured in the stator circuit. Thus, unlike existing DTC techniques, measurements are carried out at one terminal of the machine whereas the switching action is carried out at another terminal. Here the directly-controlled quantities are the stator active and reactive powers; hence, the algorithm is referred to as *direct power control* in the text. The proposed algorithm also differs from conventional DTC in that it does not use integration of PWM voltages. Hence, it can work stably even at zero rotor frequency. The method is inherently position sensorless and does not depend on machine parameters like stator/rotor resistance. It can be applied to VSCF applications like wind power generation as well as high power drives.

The concept of direct power control is first introduced and details of the control strategy are discussed. The laboratory experimental setup on which the algorithm is implemented is described. Relevant simulation and experimental results are presented to validate the performance of the proposed method.

II. CONCEPT OF DIRECT POWER CONTROL

The basic concept of direct control of active and reactive powers can be appreciated from the phasor diagrams based on the equivalent circuit of the doubly-fed machine as shown in Fig. 2. From the phasor diagram in Fig. 3 it is noted that the component i_{sq} of the stator current has to be controlled to control the stator active power P_s and i_{sd} has to be controlled to control the stator reactive power Q_s. This is achieved in turn by controlling the rotor currents i_{rq} and i_{rd}, respectively, in conventional field oriented control strategy.

The effect of injection of these rotor currents on the air-gap and rotor fluxes can be derived by subtracting and adding the respective leakage fluxes. The variation of the rotor flux with variations in the active and reactive power demand is shown in Fig. 4(a) and (b). In Fig. 4(a) $i_{rd} = 0$, i.e., the reactive power is fed completely from the stator side. Under this condition if i_{rq} is varied from 0 to full load, the locus of $\underline{\psi}_r$ varies along A–B which indicates a predominant change in angle δ between $\underline{\psi}_s$
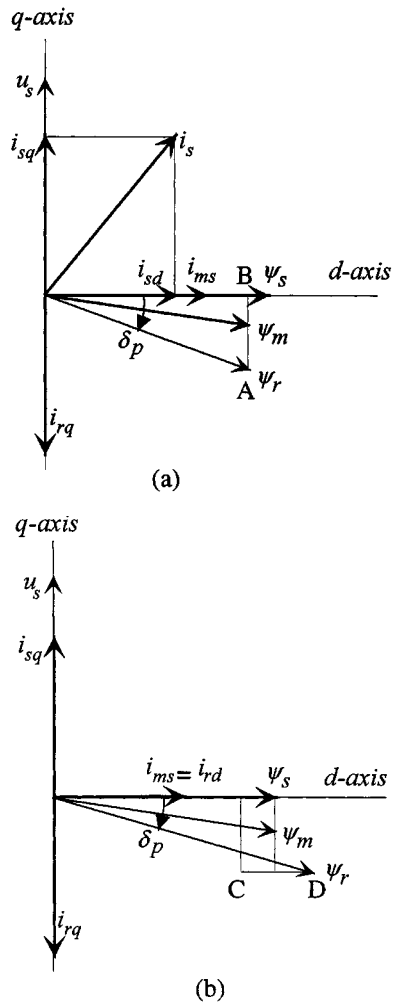
(a)

(b)

Fig. 4. Phasor diagram showing variations in rotor flux with change in active and reactive power.

(a)

(b)

Fig. 5. (a) Orientation of the rotor winding in space with respect to which the voltage space phasors are drawn and (b) voltage space phasors.

and ψ_r, whereas the magnitude of ψ_r does not change appreciably. In other words, a change in the angle δ would definitely result in a change in the active power handled by the stator in a predictable fashion.

In Fig. 4(b) the stator active power demand is maintained constant so that i_{rq} is constant and i_{rd} is varied from 0 to the rated value of i. Here the locus of ψ_r varies along C–D, resulting in a predominant change in magnitude of ψ_r, whereas the variation of δ is small. Therefore, the reactive power drawn from the grid by the stator can be reduced by increasing the magnitude of the rotor flux and vice-versa. It may be noted that the phasor diagrams as indicated in Fig. 4(a) and (b) remain the same irrespective of the reference frame; the frequency of the phasors merely changes from one reference frame to the other. It can be concluded from the above discussion that

i) The stator active power can be controlled by controlling the angular position of the rotor flux vector.

ii) The stator reactive power can be controlled by controlling the magnitude of the rotor flux vector.

These two basic notions are used to determine the instantaneous switching state of the rotor side converter to control the active and reactive power as discussed in the following section.
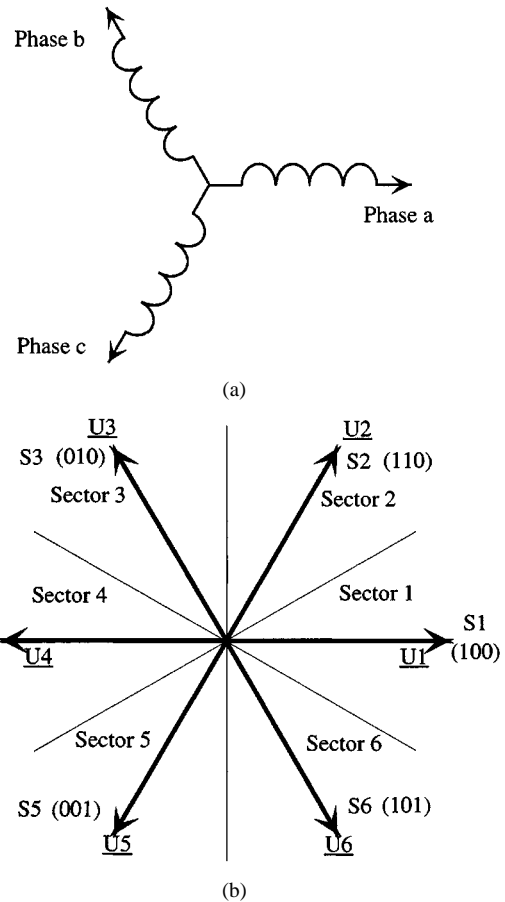
III. VOLTAGE VECTORS AND THEIR EFFECTS

Assuming that the orientation of the three phase rotor winding in space at any instant of time is as given in Fig. 5(a), the six active switching states S1, S2 $\cdots$ S6 would result in the voltage space vectors $\underline{U1}$, $\underline{U2} \cdots \underline{U6}$ [Fig. 5(b)] at that instant. In order to make an appropriate selection of the voltage vector the space phasor plane is first subdivided into six 60° sectors 1, 2... 6. The instantaneous magnitude and angular velocity of the rotor flux can now be controlled by selecting a particular voltage vector depending on its present location. The effect of the different vectors as reflected on the stator side active and reactive powers, when the rotor flux is positioned in Sector 1 is illustrated in the following subsections.

A. Effect of Active Vectors on Active Power

Considering anti clockwise direction of rotation of the flux vectors in the rotor reference frame to be positive, it may be noted that ψ_s is ahead of ψ_r in motoring mode of operation and ψ_s is behind ψ_r in generating mode. This is illustrated in Fig. 6(a) and (b) respectively. In the rotor reference frame the flux vectors rotate in the positive direction at subsynchronous speeds, remain stationary at synchronous speed and start rotating in the negative direction at supersynchronous speeds.

Assuming that the rotor flux is positioned in Sector 1, application of voltage vectors $\underline{U2}$ and $\underline{U3}$ accelerates ψ_r in the positive
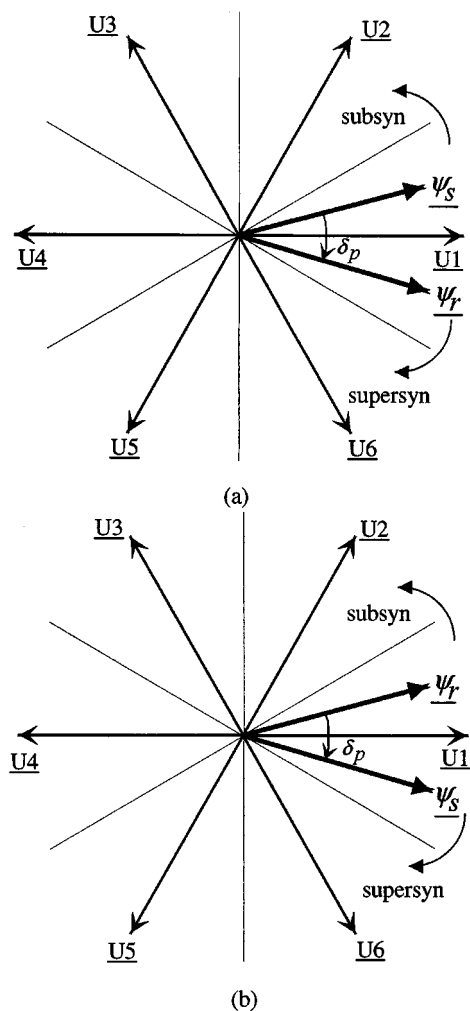
Fig. 6. Flux vectors in (a) motoring mode and (b) generating mode.

direction. In the motoring mode of operation, this reduces the angular separation between the two fluxes resulting in a reduction of active power drawn by the stator. In the generating mode of operation, application of vectors $\underline{U2}$ and $\underline{U3}$ results in an increase in angular separation between the two and thereby an increase in the active power generated by the stator. (P_s being negative for generation, application of $\underline{U2}$ and $\underline{U3}$ still results in a reduction of positive active power.) Similarly it can be seen that the effect of $\underline{U5}$ and $\underline{U6}$ on the active power would be exactly opposite to that of $\underline{U2}$ and $\underline{U3}$ in both the motoring and generating modes.

Power drawn by the stator being taken as positive and power generated being taken as negative, it may therefore, be concluded that, if the rotor flux is in the kth sector, where $k = 1, 2, 3 \ldots 6$, application of vectors $U(k+1)$ and $U(k+2)$ would result in a reduction in the stator active power and application of vectors $U(k-1)$ and $U(k-2)$ would result in an increase in the stator active power.

B. Effect of Active Vectors on Reactive Power

From the phasor diagrams Fig. 4(a) and (b) it can be seen that the reactive power drawn by the stator depends upon the component of ψ_r along ψ_s i.e., ψ_{rd}. The angle between ψ_s and ψ_r i.e., δ being small, the magnitude of ψ_r is approximately equal to ψ_{rd}. Therefore, when the rotor flux vector is located in

Sector 1, voltage vectors $\underline{U1}$, $\underline{U2}$, and $\underline{U6}$ increase the magnitude of ψ_r whereas, $\underline{U3}$, $\underline{U4}$, and $\underline{U5}$ reduce it. This holds good irrespective of whether the machine is operating in motoring or generating mode. An increase in magnitude of ψ_r indicates an increased amount of reactive power being fed from the rotor side and hence, a reduction in the reactive power drawn by the stator resulting in an improved stator power factor. A decrease in magnitude of ψ_r amounts to lowering of the stator power factor.

As a generalization it can therefore, be said that if the rotor flux resides in the kth sector, switching vectors $U(k), U(k+1)$, and $U(k-1)$ reduce the reactive power drawn from the stator side and $U(k+2), U(k-2), U(k+3)$ increase the reactive power drawn from the stator side.

C. Effect of Zero Vector on Active Power

The effect of the zero vectors is to stall the rotor flux without affecting its magnitude. This results in an opposite effect on the stator active power in subsynchronous and supersynchronous modes of operation.

In subsynchronous motoring, application of a zero vector increases δ as ψ_s keeps rotating in the positive direction at slip speed. Above the synchronous speed, ψ_s rotates in the counter clockwise direction thereby reducing δ. Hence active power drawn by the stator increases for subsynchronous operation and decreases for supersynchronous operation. Active power generated being negative, the same conclusion holds true for the generating modes as well.

D. Effect of Zero Vector on Reactive Power

Since a zero vector does not change the magnitude of the rotor flux its effect on the reactive power is rather small. Nevertheless, there is some small change in Q_s; its effect being dependent on whether the angle between the stator and rotor fluxes increases or decreases due to the application of a zero vector. An increase in angular separation between the two fluxes reduces ψ_{rd} resulting in an increment of Q_s drawn from the stator side. The converse is true when δ reduces.

It is observed that the change in Q_s due to the application of the zero vector is different in all the 4 modes of operation. This is summarized in Table I.

IV. CONTROL ALGORITHM

With the inferences drawn in the previous section it is possible to switch an appropriate voltage vector in the rotor side at any given instant of time to increase or decrease the active or reactive power in the stator side. Therefore, any given references for stator active and reactive powers can be tracked within a narrow band by selecting proper switching vectors for the rotor side converter. This is the basis of the direct power control strategy. The details of the control algorithm are discussed in the following subsections.

It should be noted that the torque reference for the machine is decided by an outer loop for either motoring or generating application. The reference for the stator power can, therefore, be calculated as

$$P_s^* = m_d^* \cdot \omega_s. \tag{1}$$

TABLE I
EFFECT OF ZERO VECTOR ON ACTIVE AND REACTIVE POWER

Speed	Motoring	Generating
Subsynchronous	$\delta_p \uparrow \Rightarrow \psi_{rd} \downarrow \Rightarrow Q_s \uparrow$	$\delta_p \downarrow \Rightarrow \psi_{rd} \uparrow \Rightarrow Q_s \downarrow$
Supersynchronous	$\delta_p \downarrow \Rightarrow \psi_{rd} \uparrow \Rightarrow Q_s \downarrow$	$\delta_p \uparrow \Rightarrow \psi_{rd} \downarrow \Rightarrow Q_s \uparrow$

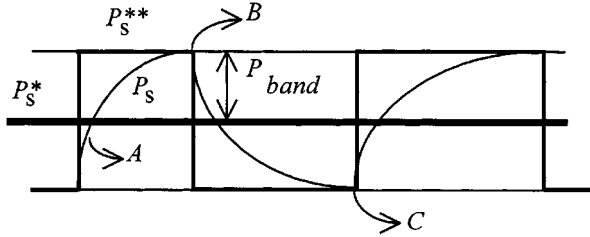Note: $\uparrow$ denotes increase, $\downarrow$ denotes decrease

Fig. 7. Hysteresis control of active power.

Q_s^* is set according to the desired power factor at the stator terminals.

A. Measurement of Stator Active and Reactive Power

The active and reactive powers on the stator side can be directly computed from the stator currents and voltages. Assuming a balanced three phase three wire system, only two currents and two voltages need to be measured. The active and reactive powers can be expressed as

$$P_s = \frac{2}{3}\left(u_{sa}i_{sa} + u_{s\beta}i_{s\beta}\right) \tag{2}$$

$$Q_s = \frac{2}{3}\left(u_{s\beta}i_{sa} - u_{sa}i_{s\beta}\right) \tag{3}$$

where

$$u_{sa} = \frac{3}{2}u_{s1} \tag{4}$$

$$u_{s\beta}\frac{\sqrt{3}}{2}\left(u_{s1} + 2u_{s2}\right) \tag{5}$$

and,

$$i_{sa} = \frac{3}{2}i_{s1} \tag{6}$$

$$i_{s\beta} = \frac{\sqrt{3}}{2}\left(i_{s1} + 2i_{s2}\right). \tag{7}$$

B. Defining References and Errors

As shown in Fig. 7, P_s^* is the reference for stator active power. The actual power P_s is to be controlled to stay within a band of width P_{band} about P_s^*. This is achieved by defining an auxiliary reference P_s^{**} and switching as per the following logic.

$$
\begin{aligned}
&P_{err} = P_s^{**} - P_s \\
&\text{if } (P_{err} > 0) \quad P_s^{**} = P_s^* + P_{band} \\
&\text{else} \qquad\qquad\quad P_s^{**} = P_s^* - P_{band}.
\end{aligned} \tag{8}
$$

In a similar manner the error and reference for the reactive power can be written as

$$
\begin{aligned}
&Q_{err} = Q_s^{**} - Q_s \\
&\text{if } (Q_{err} > 0) \quad Q_s^{**} = Q_s^* + Q_{band} \\
&\text{else} \qquad\qquad\quad Q_s^{**} = Q_s^* - Q_{band}.
\end{aligned} \tag{9}
$$

C. Switching Vector Selection

In order to determine the appropriate switching vector at any instant of time, the errors in P_s and Q_s, and the sector in which the rotor flux vector is presently residing are taken into consideration. Thus the following two switching tables for active vector selection can be generated. Tables II and III correspond to negative P_{err} and positive P_{err}, respectively.

If the rotor side converter is switched in accordance to these tables it is possible to control the active and reactive powers in the stator side within the desired error bands. But the use of active vectors alone would result in nonoptimal switching of the converter and also a higher switching frequency.

By considering the effect of the zero vector on active and reactive powers, the logic for selecting the zero vector can be summarized as in Table IV. During subsynchronous motoring mode of operation, the application of a zero vector will increase Q_s as seen from Table I. As δ_p increases under this condition, P_s also increases. Hence, when the errors in Q_s and P_s are positive, a zero vector is applied to effect an increment in both the stator active and reactive powers and thereby bring down the errors. The other entries in the table can be worked out in a similar manner. Whenever a zero vector has to be applied, the one nearest to the present active vector is selected to minimize the number of switchings.

Also, it is observed that the effect of the zero state on P_s is opposite in the subsynchronous and supersynchronous modes of operation. This criterion is used in detecting the transition from subsynchronous to supersynchronous operation and *vice-versa*.

V. SECTOR IDENTIFICATION OF ROTOR FLUX

In order to implement the switching algorithm the present sector of the rotor flux has to be identified. The exact position of the rotor flux space phasor within the sector is not of importance as far as the selection of the switching vectors is concerned.

The proposed method of sector identification is based on the direction of change in Q_s when a particular switching vector is applied. The concept is illustrated by the following example. Suppose that the present position of the rotor flux is in Sector 1 and it is moving in the positive direction (corresponding to subsynchronous operation). Therefore, application of switching states S2 and S6 results in a reduction of Q_s and application of S3 and S5 results in an increase of Q_s. When the rotor flux vector crosses over to Sector 2, the effect of states S3 and S6 on Q_s would reverse. Vector $\underline{U3}$ would now act to reduce Q_s instead of increasing it. Similarly the effect of vector $\underline{U6}$ on Q_s would also be opposite. These reversals in the direction of change of Q_s, when a particular vector is applied, can be detected and a decision for sector change may be taken on this

TABLE II
SELECTION OF ACTIVE SWITCHING STATES WHEN $(P_{err} <= 0)$

	Sector 1	Sector 2	Sector 3	Sector 4	Sector 5	Sector 6
Qerr > 0	S3	S4	S5	S6	S1	S2
Qerr <= 0	S2	S3	S4	S5	S6	S1

TABLE III
SELECTION OF ACTIVE SWITCHING STATES WHEN $(P_{err} > 0)$

	Sector 1	Sector 2	Sector 3	Sector 4	Sector 5	Sector 6
Qerr > 0	S5	S6	S1	S2	S3	S4
Qerr <= 0	S6	S1	S2	S3	S4	S5

TABLE IV
CONDITION FOR SELECTION OF ZERO VECTOR

Speed	Motoring	Generating
Subsynchronous	$Q_{err} \geq 0 \ \&\& \ P_{err} \geq 0$	$Q_{err} < 0 \ \&\& \ P_{err} \geq 0$
Supersynchronous	$Q_{err} < 0 \ \&\& \ P_{err} < 0$	$Q_{err} \geq 0 \ \&\& \ P_{err} < 0$

TABLE V
EXPECTED DIRECTION OF CHANGE IN Q_s

	S0	S1	S2	S3	S4	S5	S6	S7
Sector 1	0	-	-	+	+	+	-	0
Sector 2	0	-	-	-	+	+	+	0
Sector 3	0	+	-	-	-	+	+	0
Sector 4	0	+	+	-	-	-	+	0
Sector 5	0	+	+	+	-	-	-	0
Sector 6	0	-	+	+	+	-	-	0

TABLE VI
DIRECTION OF CHANGE OF SECTOR

	S0	S1	S2	S3	S4	S5	S6	S7
Sector 1	0	0	- 1	+ 1	0	- 1	+ 1	0
Sector 2	0	+ 1	0	- 1	+ 1	0	- 1	0
Sector 3	0	- 1	+ 1	0	- 1	+ 1	0	0
Sector 4	0	0	- 1	+ 1	0	- 1	+ 1	0
Sector 5	0	+ 1	0	- 1	+ 1	0	- 1	0
Sector 6	0	- 1	+ 1	0	- 1	+ 1	0	0

basis. Similarly, if the flux vector is rotating in the negative direction (supersynchronous operation) the effect of states S2 and S5 on Q_s would change in direction when ψ_r changes over from Sector 1 to Sector 6. Thus in any particular direction of rotation there are two vectors which can provide the information for a change in sector. Since the rotor flux vector cannot jump through sectors the change will always be by one sector, either preceding or succeeding. In this method, even though the exact position of the flux is unknown, the sector information can be updated just by observing the changes in Q_s due to the applied vectors. It may be noted that the effect of the vectors on P_s would not provide a conclusive inference about the change in sector.

The expected direction of change in Q_s due to the application of any switching state in the different sectors can be summed up as shown in Table V. It may however, be noted that in a particular sector not all vectors will be applied. For example, in sector k,

vectors $U(k)$ and $U(k + 3)$ will never be applied. These vectors would have predominant effect on the reactive power, but their effect on the active power would depend on the actual position of the rotor flux vector in the sector. In most applications there is hardly any requirement for fast transient changes in reactive power; so it is not necessary to apply the strongest vector to effect any change in Q_s. In the switching logic, therefore, only those vectors are selected which have uniform effects on P_s and Q_s in terms of their direction of change irrespective of the position of the rotor flux in a particular sector.

For any given vector applied in a particular sector the expected direction of change in Q_s can be read off from Table V. The actual direction of change can be computed from the present value of Q_s and its previous value. If the actual direction of change is opposite to the expected direction of change then a decision on change of sector is taken. Whether the sector change has to be effected in the clockwise or anti clockwise direction
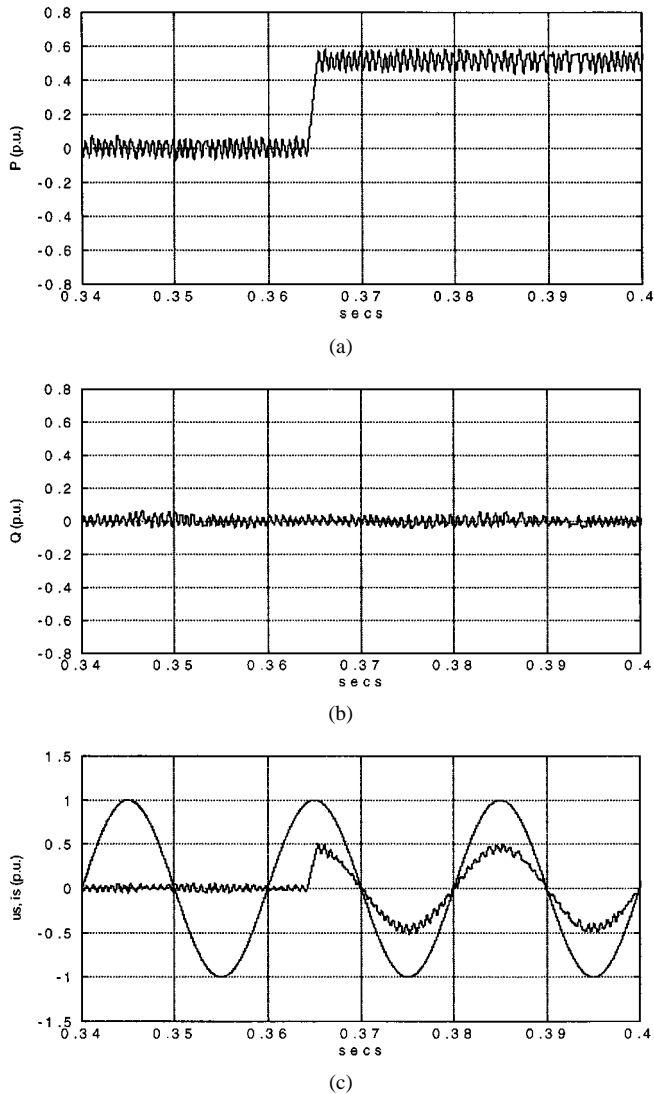
Fig. 8. Simulation results showing transient responses of P_s, Q_s and corresponding i_s due to step change in P_s^* from 0 to 0.5 p.u. with $Q_s^* = 0$ at $\omega = 0.9$ p.u., (a) response of P_s, (b) response of Q_s, and (c) response of i_s.

Fig. 9. Simulation results showing transient responses of P_s, Q_s and corresponding i_s due to step change in P_s^* from 0 to -0.5 p.u. with $Q_s^* = 0$ at $\omega = 0.9$ p.u., (a) response of P_s, (b) response of Q_s, and (c) response of i_s.

depends on the applied vector and the observed change in Q_s. This information is stored in another lookup table (Table VI).

The method of sector identification is therefore, independent of any machine parameter but relies on directly measurable fixed frequency quantities. It is also independent of the rotor frequency and can work stably at or near synchronous speed.

VI. SIMULATION RESULTS

The direct power control algorithm is simulated on the MATLAB-SIMULINK platform. The transient response due to a step change in active power command P_s^* from 0 to 0.5 p.u., while Q_s^* is maintained at 0 is shown in Fig. 8(a) and (b). P_{band} and Q_{band} are kept at 0.05 p.u. in this case. It is observed that P_s reaches its set value in approximately 2 ms. This can be the fastest possible response at a given speed because only the desired active vector is used during the transient. The response of the stator current corresponding to this step change in active power is presented in Fig. 8(c). Since the reactive power reference Q^* is held at zero, unity power factor operation is clearly
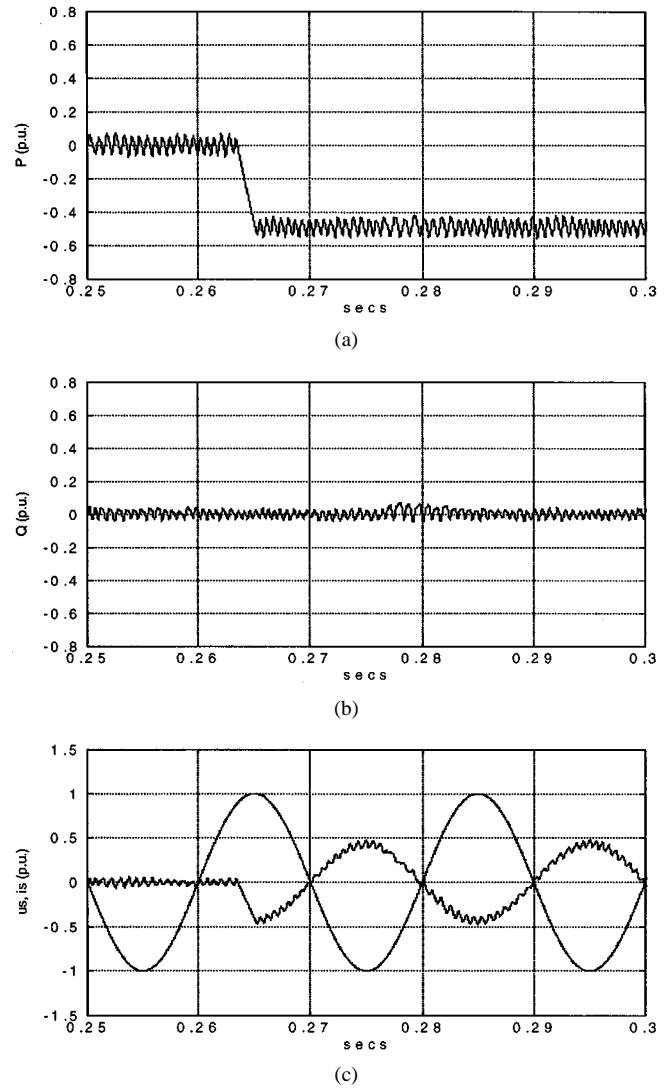
observed at the stator terminals. Similar transient response for generating condition is given in Fig. 9(a)–(c).

## VII. IMPLEMENTATION AND EXPERIMENTAL RESULTS

The schematic block diagram of the laboratory experimental setup is given in Fig. 1. It consists of a 3.5 kW wound rotor induction machine with its stator connected to the 415 V, 50 Hz, 3-ϕ power grid, and the rotor being fed by two back-to-back IGBT-based PWM converters. The setup is organized for generation operation where the torque-speed characteristics of the prime mover (such as a wind turbine) are simulated by a 5 hp dc motor driven by a commercial four-quadrant thyristor drive. A *TMS320F240* DSP based digital control platform is designed and employed for implementing the direct power algorithm. The processor runs at a clock frequency of 36 MHz and the sampling frequency used is 56 μs. The software is assembly coded for fast real-time execution. For the sake of easy uniformity, the oscilloscope waveforms presented in this section are scaled in such a manner that 5 V represents 1 p.u.
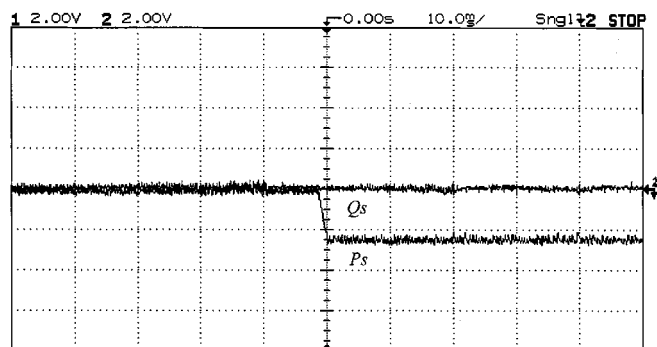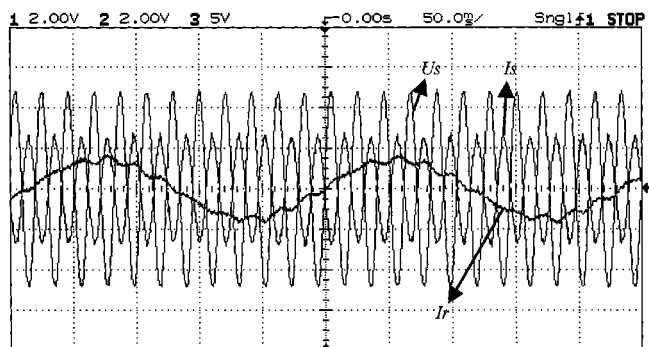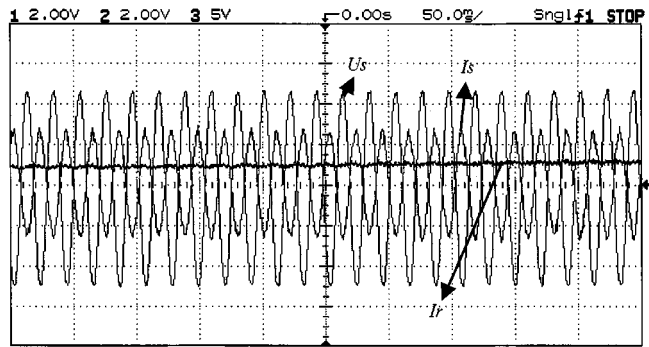
(a)
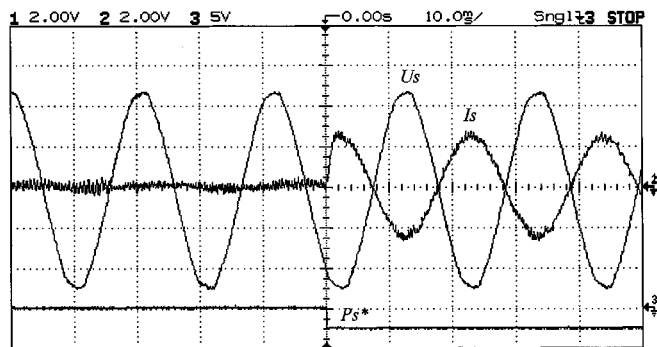
(b)
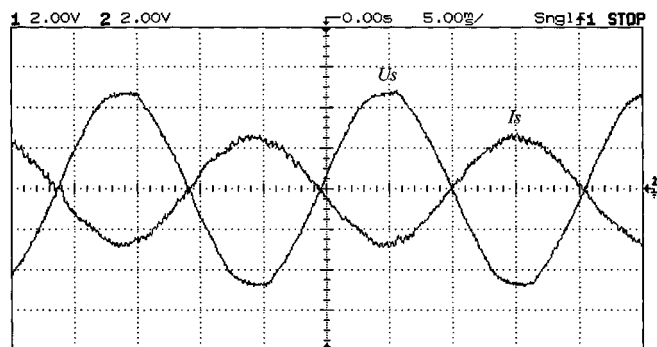
(c)

Fig. 10. (a) Experimental waveforms showing transient response of P_s and Q_s due to step change in P_s^* from 0 to -0.5 p.u. and $Q_s^* = 0$. (b) Experimental waveforms showing transient response of i_s due to step change in P_s^* from 0 to -0.5 p.u. and $Q_s^* = 0$. (c) Experimental waveforms showing steady-state waveforms of i_s and u_s.

(a)

(ab)

Fig. 11. (a) Experimental results showing steady-state waveforms u_s, i_s, i_r for $P_s^* = -0.5$ p.u., $Q_s^* = 0$ at 1300 rpm (subsynchronous operation). (b) Experimental results showing steady-state waveforms u_s, i_s, i_r for $P_s^* = -0.5$ p.u., $Q_s^* = 0$ at 1430 rpm (synchronous operation).
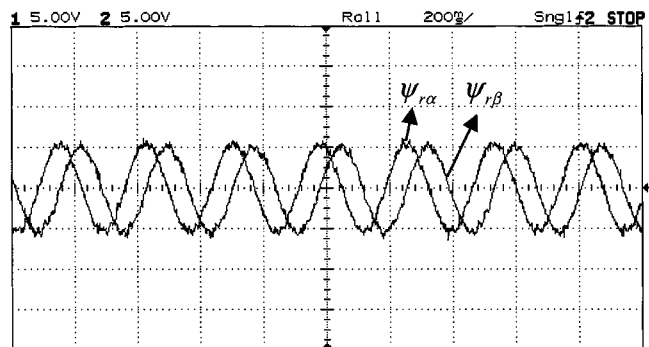

Fig. 12. Experimental results showing steady-state ψ_{ra}, $\psi_{r\beta}$ for $P_s^* = -0.25$ p.u., $Q_s^* = 0$.

Transient in active power for a step change in P^* from 0 to -0.5 p.u. is shown in Fig. 10(a). Q^* is maintained at 0. As P^* is changed P_{err} goes out of the prescribed band of 0.05 p.u. This results in the selection of only the active vectors thereby effecting the fastest possible change in P^*. The rate of change of P_s is decided by the rate of change of rotor current which in turn depends on the dc link voltage. It may be noted from these waveforms, that, the transient responses in P_s and Q_s are perfectly decoupled. The steady-state ripple in P_s and Q_s due to switching between the positive and negative error bands can also be observed. Fig. 10(b) illustrates the effect of the active power transient as reflected in the stator current waveform. The steady-state current waveform in Fig. 10(c) clearly shows unity power factor operation.

The steady-state stator voltage and current waveforms for subsynchronous and synchronous operation are given in

Fig. 11(a) and (b) respectively. The synchronous speed operation is observed to be perfectly stable. In Fig. 12, the steady-state rotor flux waveforms ψ_{ra} and $\psi_{r\beta}$ are presented.

Fig. 13(a) shows the steady-state waveforms of P_s and Q_s along with the sector information for $P_s^* = -0.5$ p.u. and $Q_s^* = 0$. (The sector information is scaled and output through DAC such that the analog output voltage is 1 V multiplied by the sector number.) For reliable detection of the direction of change of Q_s a minimum switching period of six sampling periods (336 μs) of a particular switching state is maintained. This also puts a maximum switching limit of 4.5 kHz for the rotor side converter.

Fig. 13(b) gives the rotor current waveform along with the sector information for transition through synchronous speed. During subsynchronous speed operation, the flux vectors rotate in the positive direction in the rotor reference frame; hence
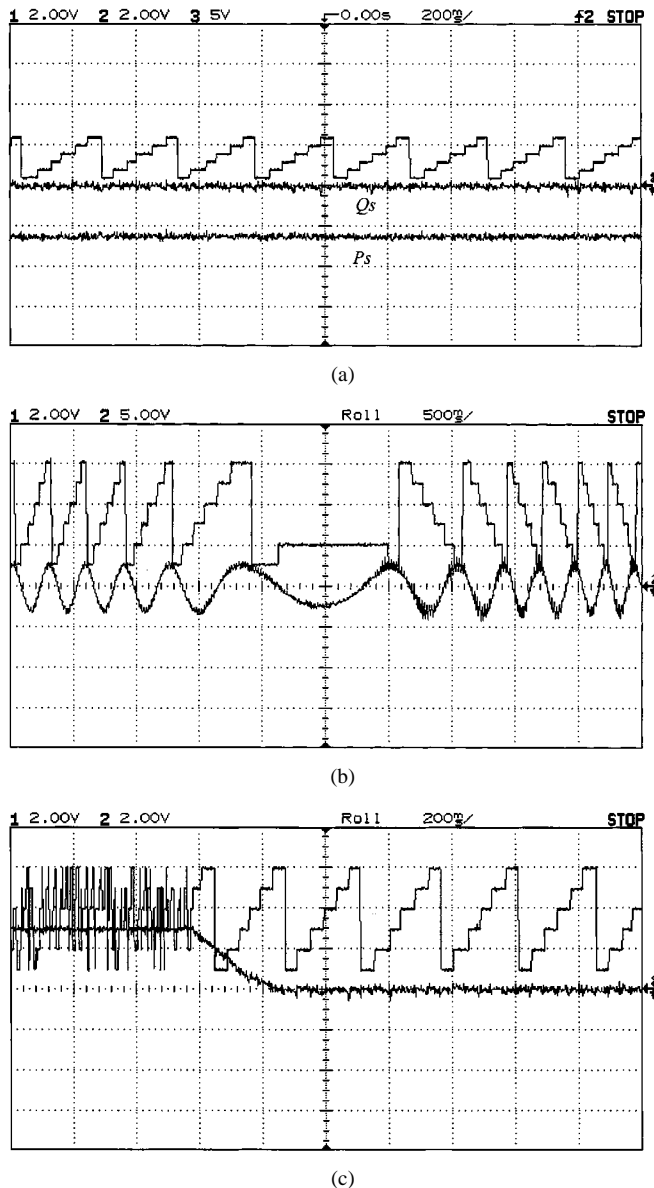
(a)

(b)

(c)

Fig. 13. (a) Experimental results showing P_s, Q_s and sector information during steady-state operation with $P_s^* = -0.5$ p.u., $Q_s^* = 0$ at 1300 rpm. (b) Experimental results showing i_r and sector information during transition through synchronous speed. (c) Experimental results showing Q_s and sector information during starting.

the sector number increases from 1 to 6 and resets back to 1. This is represented by the ascending staircase waveform. As the rotor moves over to supersynchronous speed the flux vectors start rotating in the negative direction. Therefore, the sector number changes in the reverse order as seen by the descending staircase. The changeover from subsynchronous to supersynchronous speed is observed to be smooth without any transients in the rotor current waveform.

One of the important requirements for VSCF systems with restricted speed range is that the machines have to be "cut-in" when the shaft speed crosses a given limit. This is particularly important for applications like wind power generation. Before the rotor converter is switched on the entire reactive power is drawn from the stator side. Initially Q_s^* is set to the computed value of Q_s after passing it through a low-pass filter and P_s^*

is set to zero. The implication of this is that when the control is activated the rotor does not supply any active or reactive power; the machine simply floats on the bus. It is obvious that the sector computation will be incorrect before the control is released. Since the minimum switching period on the basis of which a definite decision about sector change is made is about 336 μs, the algorithm locks onto the correct sector within 1 ms (336×3) even if the actual sector is opposite to the computed sector at switch-on. The system can thus be started "on-the-fly" without any appreciable transient in rotor and stator currents. Q_{vs}^* is then slowly ramped down to zero (or any other reference) and the desired value of P_s^* can be applied. The relevant waveforms of Q_s and the computed sector are given in Fig. 13(c).

VIII. CONCLUSION

The proposed method is thus capable of controlling the active and reactive powers of a wound rotor induction machine without rotor position sensors. It offers excellent dynamic response and decoupled control of active and reactive powers as demonstrated by the simulation and experimental results. Since it depends only on voltage and current measurements on the stator side, it is insensitive to the parameters of the machine. The method used for identification of the sector in which the rotor flux is located avoids integration of PWM voltages and consequent errors. It can start "on-the-fly" and runs stably even at zero rotor frequency. The implementation of the algorithm on a digital controller is easy because of computational simplicity. The switching information is contained in small tables and therefore, the memory utilization is also economical. All these factors make the direct power control algorithm an attractive proposition for high performance sensorless control of wound rotor induction machines in industrial drives and VSCF applications like wind power generation.

REFERENCES

[1] W. Leonhard, *Control of Electrical Drives*. New York: Springer-Verlag, 1985, ch. 13.
[2] R. Pena, J. C. Clare, and G. M. Asher, "Doubly fed induction generator for back-to-back PWM converters and its application to variable-speed wind-energy generation," *Proc. Inst. Elect. Eng.*, pt. B, vol. 143, pp. 231–241, May 1996.
[3] L. Xu and W. Cheng, "Torque and reactive power control of a doubly fed induction machine by position sensorless scheme," *IEEE Trans. Ind. Applicat.*, vol. 31, pp. 636–642, May/June 1995.
[4] R. Datta and V. T. Ranganathan, "Decoupled control of active and reactive power for a grid-connected doubly-fed wound rotor induction machine without position sensors," in *Proc. Conf. Rec. 1999 IEEE/IAS Anu. Meeting*, 1999, pp. 2623–2630.
[5] L. Morel, H. Godfroid, A. Mirzaian, and J. M. Kauffmann, "Double-fed induction machine: Converter optimization and field oriented control without position sensor," *Proc. Inst. Elect. Eng.*, pt. B, vol. 145, pp. 360–368, July 1998.
[6] E. Bogalecka, "Power control of a double fed induction generator without speed or position sensor," in *Proc. Conf. Rec. EPE Brighton*, vol. 8, ch. 50, 1993, pp. 224–228.
[7] M. Depenbrock, "Direct self control (DSC) of inverter-fed induction machine," *IEEE Trans. Power Electron*, vol. 3, pp. 420–429, Oct. 1988.
[8] I. Takahashi and T. Noguchi, "A new quick response and high efficiency control strategy of an induction motor," *IEEE Trans. Ind. Applicat.*, vol. IA-22, pp. 820–827, Sept./Oct. 1986.
[9] I. Takahashi and Y. Ohmori, "High performance direct torque control of an induction motor," *IEEE Trans. Ind. Applicat.*, vol. 25, pp. 257–264, Mar./Apr. 1989.

[10] R. Datta and V. T. Ranganathan, "Method for direct control of active and reactive power from the rotor side for a grid connected doubly-fed slip-ring induction machine without position encoder," Indian Patent 797/MAS/99, June 8, 1999.

[11] R. Datta, "Rotor side control of grid-connected wound rotor induction machine and its application to wind power generation," Ph.D dissertation, Dept. Elect. Eng., Indian Inst. Sci., Bangalore, India, Feb. 2000.

V. T. Ranganathan (SM'84) received the B.E. and M.E. degrees in electrical engineering from the Indian Institute of Science (I.I.Sc.), Bangalore, and the Ph.D. degree from Concordia University, Montreal, QC, Canada.

He joined the Electrical Engineering Department, I.I.Sc., in 1984 and is currently a Professor. His research interests are in the area of power electronics and motor drives. He has published several papers in the areas of vector control of ac drives, pwm techniques, split phase induction motor drives, and rotor side control of slip ring induction motors. He is also a consultant to industry in the above areas and has participated in a number of projects.

Dr. Ranganathan received the Prize Paper Award of the IEEE-IAS Static Power Converter Committee and the Tata Rao Prize of the Institution of Engineers India. He is a fellow of the Institution of Engineers, India.

Rajib Datta received the B.E. degree in electrical engineering from Jadavpur University, Calcutta, in 1992, the M.Tech. degree in electrical engineering from the Indian Institute of Technology, Kharagpur, in 1994, and the Ph.D. degree from the Department of Electrical Engineering, Indian Institute of Science, Bangalore, in 2000.

From January 1995 to July 2000, he was a Research Scholar in the Department of Electrical Engineering, Indian Institute of Science, Bangalore. Presently, he is a Research Scientist at ABB, Corporate Research Center, Heidelberg, Germany. His research interests include power electronics, motor drives, and wind power generation.